Journal of Rehabilitation in Civil Engineering 10-2 (2022) 35-55

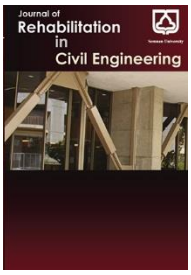

journal homepage: http://civiljournal.semnan.ac.ir/

Optimal Seismic Design of 2D Steel Moment Frames with Set-back in Height Based on Structural Performance

Arezoo Asaad Samani[1], Mohammad Ali Fathali[1], Seyed Rohollah Hoseini Vaez[1*]

1. Department of Civil Engineering, Faculty of Engineering, University of Qom, Qom, Iran
Corresponding author: hoseinivaez@qom.ac.ir

ARTICLE INFO

Article history:
Received: 07 April 2021
Revised: 26 June 2021
Accepted: 26 June 2021

Keywords:
Performance-based design;
Height irregularities;
2D steel moment frame;
Optimization;
Meta-heuristic algorithms.

ABSTRACT

Structural height set-back is a particular type of irregularity that affects the performance of the structure significantly. Therefore, researchers have always been interested in the effects of height irregularities on the seismic performance of such structures. The present study aimed to provide an optimal design based on the seismic performance of three- and nine-story steel moment frames with set-back in height. The study proposes a method that takes the acceptance criteria into account by analysis in two directions for the optimal design of steel moment frames with setbacks. Optimization in the present study aims to reduce the structural weight and obtain uniform inter-story lateral drift distribution through the acceptance criteria for each performance level. The optimization process is performed using meta-heuristic algorithms of Accelerated Water Evaporation Optimization and Accelerated Water Evaporation Optimization. The results show the efficiency of algorithms to finding the optimal solution and the appropriateness of the proposed procedure.

1. Introduction

Today, the optimum design of structures has become much more important for engineers, resulting in proposing different methods to achieve the optimal structural designs. Optimal design of structures leads to the selection of the most suitable design and reduces construction costs while also meeting the existing limitations. Various numerical methods are currently proposed to solve optimization problems; however, it is not possible to use numerical methods in some optimization problems with complex functions. Thus, researchers are interested in the application of random methods and

How to cite this article:
Asaad Samani, A., Fathali, M., Hoseini Vaez, S. (2022). Optimal Seismic Design of 2D Steel Moment Frames with Set-back in Height Based on Structural Performance. Journal of Rehabilitation in Civil Engineering, 10(2), 35-55.
https://doi.org/10.22075/jrce.2021.23082.1496

targeted search to solve these types of problems. These methods solve problems by simulation and inspiration from nature. Meta-heuristic algorithms are among the methods widely used in engineering sciences and welcomed by many researchers in solving optimization problems [1-13]. These algorithms are significantly capable of solving many complex problems and are used to find optimal answers in a short time. They also have solutions to escape the local optimum and solve the problem with sufficient speed and accuracy by providing a global solution. The seismic performance-based design of structures is one of the most common discussions in the earthquake and structural engineering sciences, currently studied by many researchers. Performance-based design (PBD) is an engineering approach to designing building elements according to the desired performance objectives. In the performance-based design of structures, designers consider different performance levels and damages against various levels of seismic risk and design the structure in such a way that the maximum deformations remain within the desired limits during an earthquake; This leads to a more accurate study of structural behavior after experiencing seismic displacement. The results of such studies can help to evaluate the real response of building systems along with their effects on the performance of buildings and improve the behavior of the structure. The following are examples of research conducted in this field. Gholizadeh et al. considered the target displacement equation according to FEMA356 and developed optimum design of steel frames using metaheuristic algorithms. The authors performed structural control for gravity loads as a prerequisite constraint before the design and optimization of the structure [14]. Kaveh et al. investigated the seismic performance-based design of the moment frames for OP, IO, LS, and CP performance levels and considered inter-story drift as the design criterion. They performed nonlinear static analysis using semi-rigid connection equations with the base shear as their criterion to determine the performance levels [15]. Gholizadeh et al. first examined the target displacement to determine the performance levels. This displacement was calculated using the equation in FEMA 356 based on the bilinearization of the pushover curve. The strength of the elements and the lateral drift of the stories were the controls performed to evaluate the structure. This study controlled the structure against the gravity load, after which the pushover analysis was carried out [16]. Gholizadeh and Poorhosseini studied the optimum PBD of steel bracing frames. They used nonlinear static analysis at different performance levels based on the displacement coefficient method of FEMA356 [17] and exposed the structure to a certain distribution of lateral loads according to this method to achieve the target displacement [18]. Also, Gholizadeh and Baghchevan performed the optimum PBD of steel frames. The strength and geometric constraints were first controlled under gravity loads, and in the case of satisfactory strength and geometric controls, pushover analysis was performed to evaluate the maximum inter-story drift as another constraint [19]. Mansoori et al. provided an optimal performance-based seismic design for concentrically braced frames at IO and CP performance levels. They considered minimizing the structural weight as the objective function and the inter-story drift ratios as the constraints of their optimization problem [20]. Gholizadeh and Fatahi used a PBD method for steel moment frames to

minimize the overall cost of structures. They primarily aimed to provide a method of seismic damage control in the framework of performance-based optimum design of steel moment frames [21]. Karimi and Hosseini Vaez carried out performance-based design optimization of 2D steel frames. They first investigated the limit state method and then performed pushover analysis of the structure at four performance levels and considering four target displacements [22]. Fathali and Hosseini Vaez investigated the performance-based optimum design of the eccentrically braced frames. They first proposed a method to model the link beams of the eccentrically braced frames, based on which the performance of the link beams could be evaluated. Then, the optimization problem was defined according to the acceptance criteria of the PBD method. Finally, they carried out the optimal design of two eccentric braced frames using meta-heuristic algorithms to investigate the feasibility of optimization based on the defined problem [23]. Gholizadeh et al. conducted a performance-based optimum design for concentrically braced frames and examined their seismic collapse capacity [24]. In addition to these studies, several other studies have been conducted in the field of performance-based design of steel frames [25-31]. The types of irregularity in structures affect the seismic behavior of them [32, 33]. The seismic performance of structures has currently received more attention from engineers due to the increase in structural irregularities resulting from architectural considerations and the specific type of structural use. The structure with a set-back in height is a special kind of irregularity that affects the performance of the structure significantly. The present study aims to provide a performance-based optimum design of three- and nine-story steel moment frames with set-back in height. Target displacement is the criterion for determining performance levels and calculated using the equation in FEMA356 based on the bilinearization of the pushover curve. The acceptance criteria of the steel moment frame have been considered according to FEMA356 at each performance level to define the constraints. Also, the nonlinear static analysis is the basic method of structural analysis, and OpenSees has been used to carry out analyses. Optimization in the present study aims to reduce the structural weight and obtain uniform inter-story lateral drift distribution by considering the acceptance criteria for each performance level. The optimization process is performed using WEO and AWEO algorithms.

2. Performance-Based Optimum Design

2.1. PBD method

The method of designing structures based on their performance, which today is preferred by structural designers compared to other design methods, is rapidly being studied and developed. The concepts of PBD method are based on the concepts of structural performance evaluation, which are expressed in the instructions for seismic rehabilitation of existing structures; In fact, the purpose of using this method is to design structures with predictable performance in the event of the earthquake. Therefore, the level of damage and performance of structural and non-structural components are determined for design engineers. In this design method first, the constraints for the performance of the structure are considered as the performance levels, and then the structure is designed such that it can satisfy these constraints under a

certain level of seismic hazard. For the performance-based design of a structure, one or more objectives can be considered as general design objectives, each goal involving the selection of a performance level and a seismic hazard level. In the current study, the immediate occupancy (IO), life safety (LS), and collapse prevention (CP) performance levels were considered from FEMA-356 at 20%, 10%, and 2% earthquake probability over 50 years, respectively. Because the nonlinear static analysis method was used to analyze the structure, the lateral loads are applied to the structure in several steps until the displacement of the control point reached the target displacement. The exact amount of target displacement at each performance level can be determined using Eq. (1) of FEMA-356, which is based on a confirmed procedure for the nonlinear response of the structure.

$$\delta_t = C_0 C_1 C_2 C_3 S_a \frac{T_e^{\,2}}{4\pi^2} g \tag{1}$$

where C_0, C_1, C_2, and C_3 are the coefficients related to simulation of nonlinear structure behavior according to FEMA-356. S_a is the spectral acceleration calculated for each performance level at 5% damping using Eq. (2). T_e is the effective fundamental period of the structure, which is calculated according to Eq. (3), and g is the acceleration of gravity.

$$S_a^k = \begin{cases} F_a S_s^k \left(0.4 + 3T_e/T_0\right) & 0 < T_e \le 0.2T_0^k \\ F_a S_s^k & 0.2T_0^k < T_e \le T_0^k \\ F_v S_1^k / T_e & T_e > T_0^k \end{cases} \tag{2}$$

$$T_0^k = (F_v S_1^k)/(F_a S_s^k), \quad k = IO, LS, CP$$

In Eq. (2), S_S and S_1 are the response acceleration parameters for a short-period (0.1 sec) and for a 1-sec period, respectively; F_a and F_v are the site class coefficients based on FEMA-356.

$$T_e = T_i \sqrt{\frac{K_i}{K_e}} \tag{3}$$

where K_i and K_e are the elastic stiffness and the effective stiffness of the structure, respectively. T_i is the fundamental elastic period. These parameters were obtained from the idealized force-displacement curve based on FEMA-356.

2.2. Optimization process

2.2.1. Formulation of Optimization Problem

One of the most important design characteristics is the construction cost of the structure, which less of it leads to a more optimized design. The goal of optimum design is to choose the best design from the acceptable ones. Each optimization problem consists of three parts: objective function, constraints and design variables. In general, an optimization problem can be formulated as:

$$\begin{aligned} &\text{Find: } \mathbf{X} = \{x_1, x_2, x_3, ..., x_{NG}\}^T \\ &\text{Minimize: } F(\mathbf{X}) = F_1(\mathbf{X}) + F_2(\mathbf{X}) \\ &\text{Subject to: } g_C(\mathbf{X}) \le 0, \ C = 0,1,2,...,NC \end{aligned} \tag{4}$$

where $\mathbf{X}$ is the vector of the design variables, $F(\mathbf{X})$ is the objective function, $g_C(\mathbf{X})$ is the C^{th} design constraint, and NC is the number of constraints. In the current study, the design variables were selected from W-shaped steel sections according to the AISC design manual [34]. According to Eq. (4), the objective function consists of two-terms [35]; F_1 is the normalized building weight as shown in Eq. (5).

$$F_1(\mathbf{X}) = \frac{1}{W_{\max}} \sum_{k=1}^{NG} \rho_k A_k \sum_{r=1}^{NM} L_r \tag{5}$$

where $W_{\max}$ is the maximum weight of the structure that is obtained by selecting the

heaviest possible section of the final section list for element groups, *NM* is the number of structural elements that are collected in *NG* design groups, ρ_k and A_k are the weight of the unit volume and cross-sectional area of the k^{th} group section, respectively, and L_r is the length of the r^{th} element in the k^{th} group. In the current study, in addition to minimizing the weight of the structure, the uniform inter-story drift distribution was also investigated. If the inter-story drift distribution is uniform, the structure will experience less damage. In Eq. (4), F_2 is the second term of the objective function for considering this problem and can be formulated as:

$$F_2(\mathbf{X}) = \left[\frac{1}{NS} \sum_{S=1}^{NS-1} \left(\frac{\upsilon_S^{CP}(\mathbf{X})/H_S}{\Delta^{CP}(\mathbf{X})/H} - 1 \right)^2 \right]^{1/2} \tag{6}$$

where *NS* is the number of structural stories, *H* is the height of the structure, and H_S is the vertical distance from the base of the structure to story *S*. Δ^{CP} and υ_S^{CP} are the roof drift and the drift of story *S* at the CP performance level, respectively. According to FEMA-356 for steel moment frames, the flexural behavior of the beams should be deformation-controlled. In steel columns, whenever the axial force is less than 50% of the lower-bound axial compression strength of the column (P_{CL}), the flexural and axial behavior of the column should be deformation-controlled and force-controlled, respectively. The behavior of plastic hinges in the steel moment frames is one of the important issues that has been studied in the type of structural systems [36]. The constraint corresponding to the plastic rotation of plastic hinges is defined as:

$$g_{i,d}^{\theta} = \left(\left| \theta_{P,d}{}^{i} \right| / \theta_{all,d}{}^{i} \right) - 1 \le 0 \quad i = IO, LS, CP \ , \ d = 1,2,...,nh \tag{7}$$

where $\theta_{P,d}{}^{i}$ and $\theta_{all,d}{}^{i}$ are the plastic rotation of the d^{th} plastic hinge and its allowable values at the i^{th} performance level based on FEMA-356, respectively, and *nh* is the number of plastic hinges. In steel columns with axial compressive forces that are more than 50% of the P_{CL}, both the axial loads and flexure should be force-controlled. According to FEMA-356, the constraint for such columns at the CP performance level is:

$$g_j^s = \left[\left(P_{UF,j} / P_{CL,j} \right) + \left(M_{U,j} / M_{CL,j} \right) \right] - 1 \le 0 \quad for \ P_{UF,j} / P_{CL,j} > 0.5 \ , \ j = 1,2,...,nf \tag{8}$$

where g_j^s is the strength constraint of the j^{th} column, *nf* is the number of columns, $P_{UF,j}$ and $M_{U,j}$ are the axial force and a bending moment of the j^{th} column derived from analysis, respectively, and $M_{CL,j}$ is the lower-bound flexural strength of the j^{th} column. The geometric constraints were controlled according to Eq. (9) [19] for satisfying design criteria of the column-column and beam-column joints in steel structures.

$$g_{G,k} = \begin{cases} \left(b_B / b_C^{bot} \right)_k - 1 \le 0 \\ \left(h_C^{top} / h_C^{bot} \right)_k - 1 \le 0 \end{cases} , \ k = 1,...,nk \tag{9}$$

where $g_{G,k}$ is the geometric constraint of the k^{th} connection, b_B and $b_C{}^{bot}$ are the flange width of the beam and flange width of the bottom column for the k^{th} connection, respectively, $h_C{}^{top}$ and $h_C{}^{bot}$ are the depth of the top and bottom columns for the k^{th} connection, respectively, and *nk* is the number of joints. The constraint for the slenderness ratio of the column (λ) is:

$$g_j^{\lambda} = \frac{\left(K_j l_j / r_j \right)}{200} - 1 \le 0 \ , \ j = 1,2,...,nf \tag{10}$$

where K_j, l_j, and r_j are the effective length factor, unsupported length, and cross-section gyration radius of the j^{th} column, respectively. The inter-story drift constraint at each performance level is:

$$g_{j,i}^{\Delta} = \left(\Delta_j^i / \Delta_{all}^i\right) - 1 \le 0$$
$$i = IO, LS, CP \ , \ j = 1,2,...,n_s \tag{11}$$

where $\Delta_j{}^i$ and $\Delta_{all}{}^i$ are the inter-story drift of the j^{th} story and the allowable inter-story drift at i^{th} performance level, respectively. The allowable inter-story drift (Δ_{all}) was considered to be 0.012, 0.031, and 0.061 of the story height for the IO, LS, and CP performance levels, respectively [22, 37]. Finally, using the exterior penalty function method, the problem constraints are applied to the objective function and can be formulated as:

$$\varphi(\mathbf{X}, r) = F(\mathbf{X})\left(1 + r\sum_{C=1}^{NC} V_C^{\,2}\right)$$
$$V_C = \max\left\{0, g_C(\mathbf{X})\right\} \tag{12}$$

In Eq. (12), r is the positive penalty parameter, φ is the pseudo-objective function, and V_C is the violation of the C^{th} constraint.

2.2.2. Metaheuristic algorithms

In this study, two metaheuristic algorithms proposed by Kaveh and Bakhshpoori [38, 39] were used to perform the optimization problems. Among these two algorithms, called Accelerated Water Evaporation Optimization (AWEO) and Water Evaporation Optimization (WEO), AWEO has a higher convergence speed and more appropriate performance than WEO. Actually, the AWEO algorithm is based on the WEO algorithm, but they are slightly different during the optimization process. The WEO process performs in two independent steps. Half of the process is based on the monolayer evaporation step and the other is based on the droplet evaporation step, while the two steps are performed simultaneously in each iteration for the process of the AWEO algorithm.

2.3. Proposed procedure

The most common analysis method for evaluating seismic performance is nonlinear static analysis. In the present study, this method is the basis of structural analysis, and the lateral loading pattern was considered in accordance with the first mode shape (modal pushover analysis [40]). In this lateral loading pattern, the lateral force applied to each story was determined by the effect of the first mode on the seismic mass of the story, as shown in Fig. 1. The gravity load applied to both frames was considered to be representative of the gravity load combination.

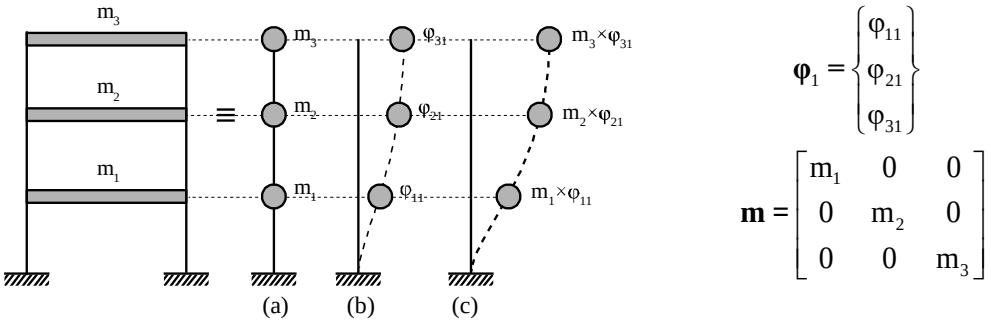

Fig. 1 The real shape of the three-story steel frame (a) Modeling frame with concentrated masses; (b) First mode shape; (c) Deformation of frame with lateral loading pattern based on the first mode.

In Fig. 1, $\boldsymbol{\varphi}_1$ and $\mathbf{m}$ are the first mode and the mass matrices of the structure. The structures considered in this study are steel moment frames with set-back in height, so the nonlinear static analysis should be performed with a lateral loading pattern based on the

first mode in two directions. Fig 2 shows the directions of the lateral loading pattern applied to the structure. The flowchart of the proposed procedure is shown in Fig. 3.

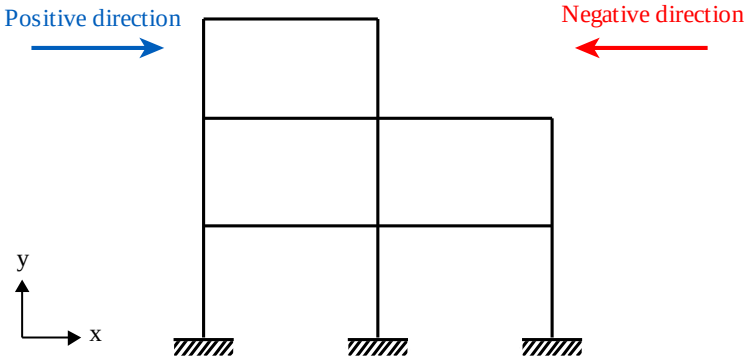

Fig. 2 The directions of the lateral loading pattern applied to the structure.

There are parameters in the target displacement equation of the flowchart in Fig. 3. The values of the parameters depend on the bilinearization behavior of the structure. On the other hand, in the process of bilinearization of the structural capacity curve, a basic assumption is needed to calculate the amount of target displacement. Therefore, there is a trial-and-error process which is considered first three initial target displacements for the roof are equal to 0.007, 0.025, and 0.05 of the total height of the structure, equivalent to IO, LS, and CP performance levels. After performing the pushover analysis, the values of members' forces, plastic hinges rotation, and drift of the stories were stored for each performance level. After recording the desired outputs from the analysis, the problem constraints are controlled according to the FEMA356 criteria for each performance level. According to the flowchart, the structure is subjected to nonlinear static analysis with lateral loading pattern based on the first mode shape in the positive direction (PD) (according to Fig. 2).

If the constraints of the optimization problem are satisfied in this stage, the nonlinear static analysis is performed with a lateral loading pattern based on the first mode shape in the negative direction (ND). There are three possible cases in this method: The constraints are not satisfied in the first stage, the constraints are satisfied in the first stage but not in the second stage, and the third case is that the constraints are satisfied in both stages. A coefficient (α) that is defined differentiates the penalty value of objective function for each case.

3. Numerical examples

Two numerical examples were considered for the PBD optimization problem of 2D steel frames with set-back in height using WEO and AWEO algorithms. The optimization process of both examples was performed in 20 independent runs. The number of population and the maximum number of iterations for each optimization algorithm were selected 60 and 300, respectively.

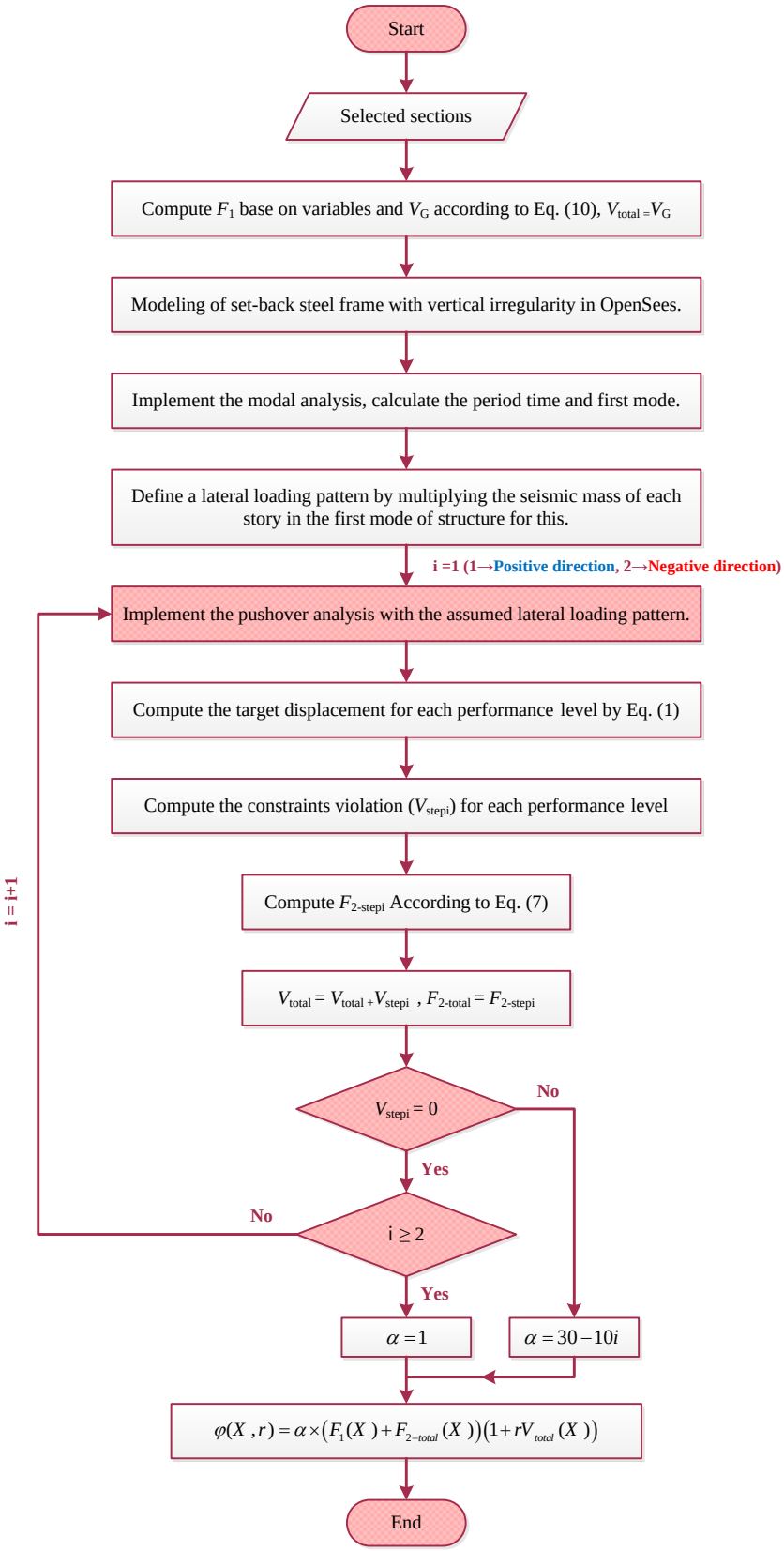

Fig. 3 Flowchart of proposed procedure.

The modulus of elasticity was assumed 2.001×10^5 MPa to solve problems. The expected yield strength (F_{ye}) of the steel for the columns and beams was considered 397 and 339 MPa, respectively. The beam section list was made by all W-shaped sections, but the column sections were selected as wide-flange sections W8 to W14. Table 1 shows the values of parameters S_1, S_S, F_a and F_v.

Table 1 Parameters for site class of D (Kaveh et al. 2010 [25]).

Performance level	Hazard level	S_s (g)	S_1 (g)	F_a	F_v
IO	20%/50-years	0.658	0.198	1.27	2.00
LS	10%/50-years	0.794	0.237	1.18	1.92
CP	2%/50-years	1.150	0.346	1.04	1.70

3.1. Three-story, four-bay steel frame

This example considers the optimization problem of a three-story steel frame with a set-back in height, as shown in Fig. 4. Grouping of elements and applied loads for the frame are shown in this Fig. The constant gravity load of W_1 = 32 kN/m was applied to the first and second stories and the constant gravity load of W_2 = 28.7 kN/m was applied to the roof beams. Fig. 5 shows the number of potential plastic hinges. The seismic weights were assumed as 4688 kN for the first and second stories and 5071 kN for the third story. The optimal sections and the best, worst, average, standard deviation and coefficient of variation of the structure weights are summarized in Table 2.

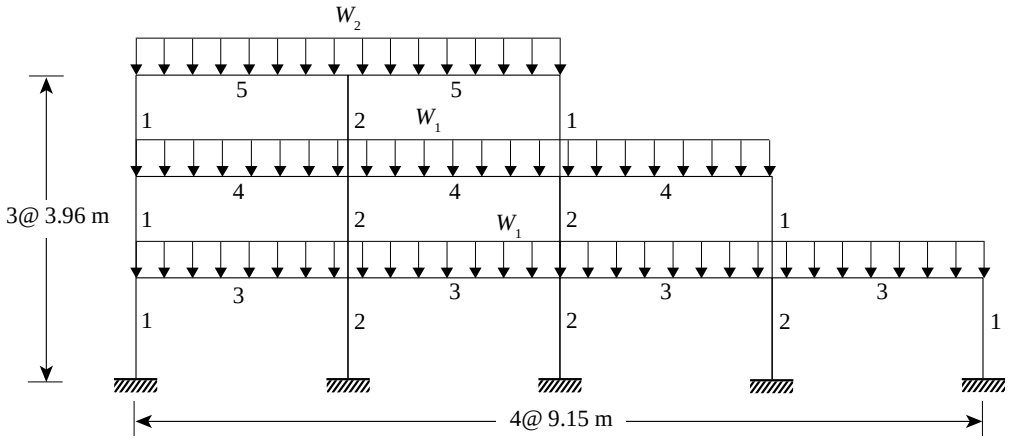

Fig. 4 Geometry, loading and grouping of the elements of three-story steel frame with set-back in height

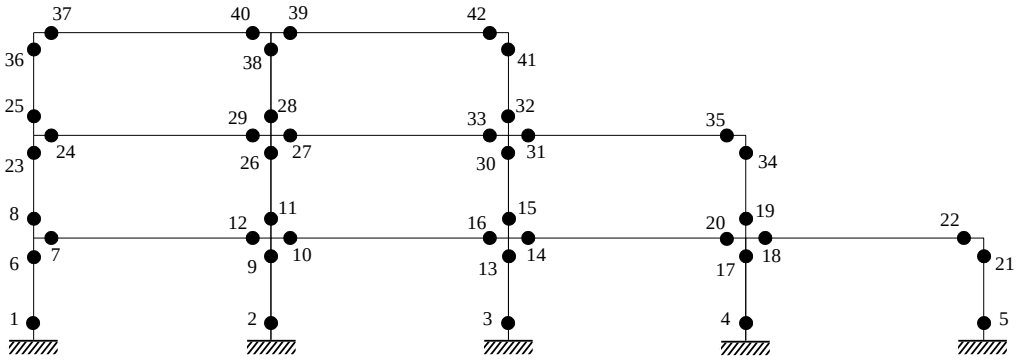

Fig. 5 Number of potential plastic hinges in three-story steel frame

Table 2 Optimal sections and weights for three-story steel frame.

Element group	WEO	AWEO
1	W12 × 87	W12 × 87
2	W14 × 90	W12 × 87
3	W14 × 48	W12 × 45
4	W27 × 84	W24 × 76
5	W12 × 30	W8 × 40
Best weight (kN)	128.95	125.44
Worst weight (kN)	264.08	294.48
Average weight (kN)	197.13	197.91
Standard deviation of weights (kN)	47.26	55.57
Coefficient of variation (%)	23.97	28.08

The ratios of the best result to those obtained from each algorithm in 20 independent runs are compared in Fig. 6. Increasing this ratio indicates that the solution obtained by the algorithm is better; because the solution achieved is less different from the best solution. Fig.6 and Table 2 demonstrate that the scattering caused by random seed in the results for each independent run of WEO is less than AWEO; thus, it has a more uniform performance.

Fig. 6 Ratio of best solution to solution of each algorithm for three-story steel frame.

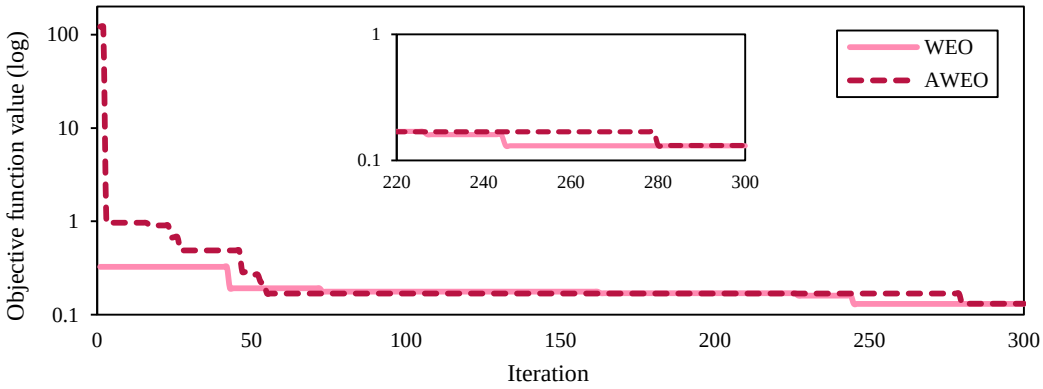

Fig. 7 Convergence curve of best solution of each algorithm for three-story steel frame.

Fig. 7 shows the convergence curve of the best solution obtained by each algorithm for a three-story steel frame with a set-back in height. Fig. 8 and 9 indicate the plastic hinge formation patterns for the optimal solution of the three-story frame with lateral loading pattern based on the first mode shape in the positive and negative direction, respectively, at IO, LS and CP performance levels. The ratios of plastic hinges rotation to their allowable values according to FEMA 356 for a three-story steel frame with lateral loading pattern in the positive and negative directions are shown in Fig. 10. These ratios were less than unity for all plastic hinges, which indicates the acceptable amounts of rotations (rotations of plastic hinges which were negligible are not shown).

Fig. 11, 12 and 13 show the displacement of stories, displacement-to-height ratio, and inter-story drift ratio of the structure for lateral loading in both directions at IO, LS and CP, respectively. Fig. 14 compares the inter-story drift ratios to their permitted values for a three-story steel frame.

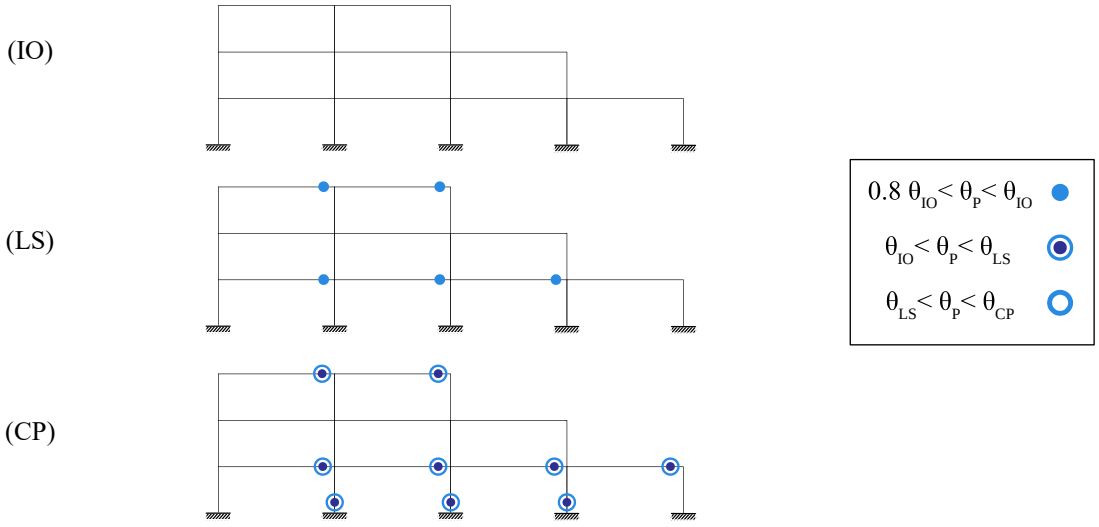

Fig. 8 Plastic hinges formation for three-story frame with lateral loading pattern in positive direction.

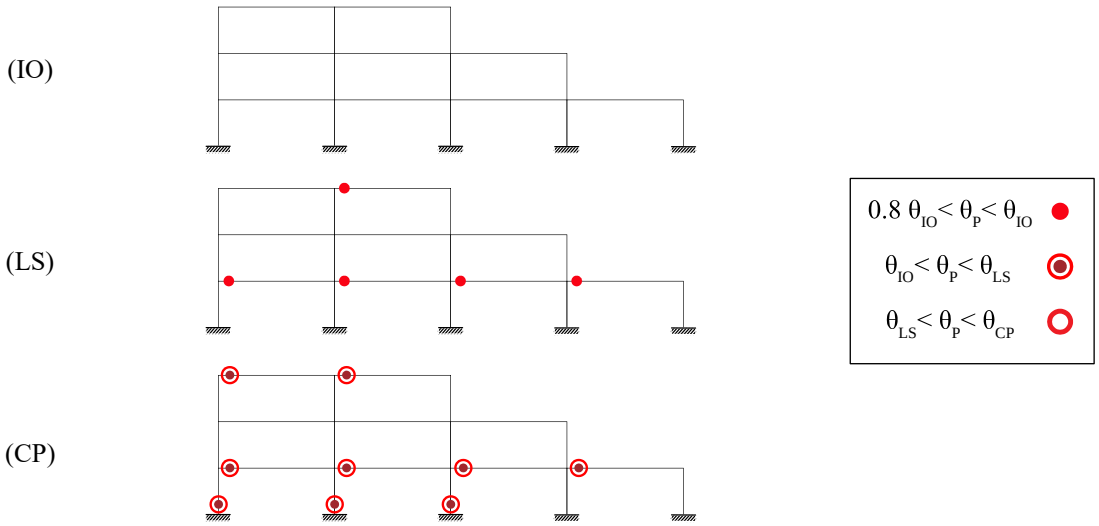

Fig. 9 Plastic hinges formation for three-story frame with lateral loading pattern in negative direction.

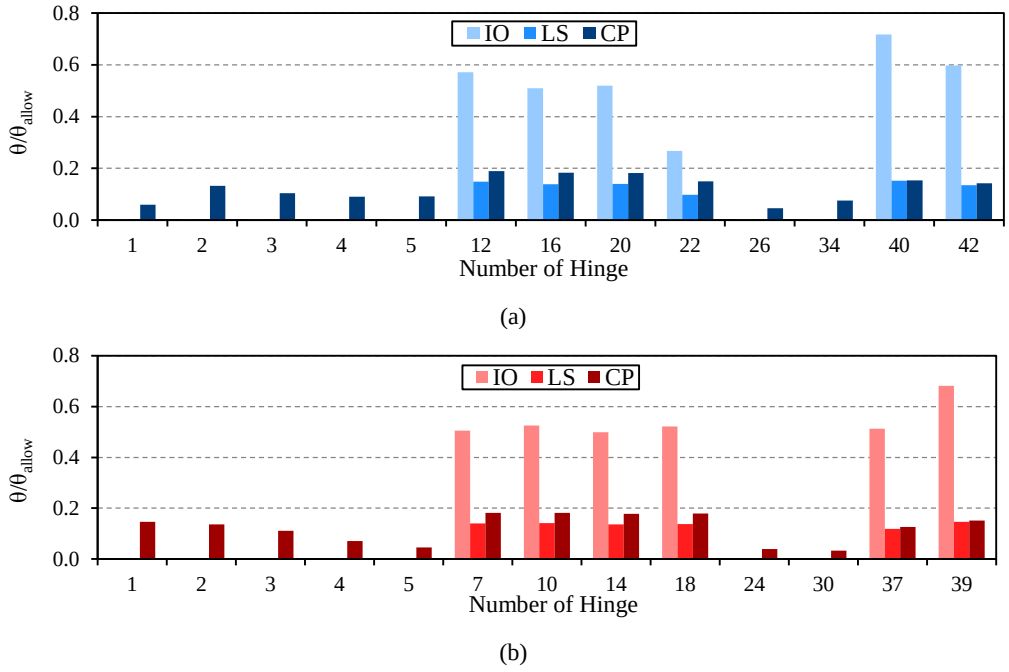

Fig. 10 Ratio of plastic hinges rotation to their allowable values for three-story steel frame with lateral loading pattern in: (a) positive direction; (b) negative direction.

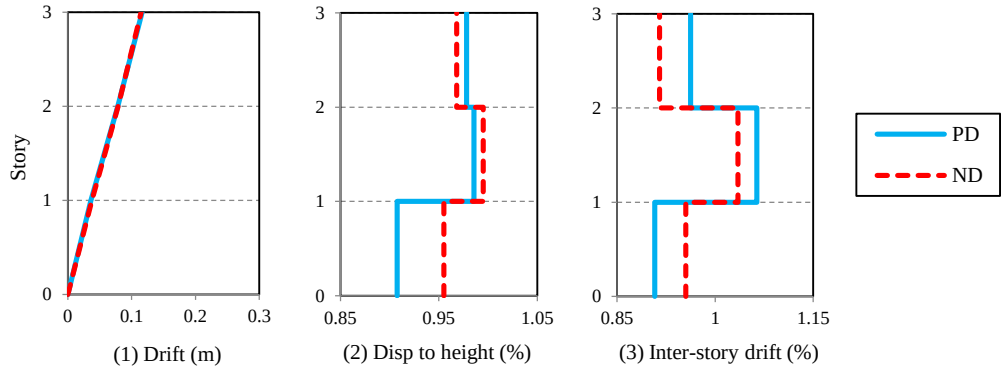

Fig. 11 Results of story drift for three-story steel frame with lateral loading pattern in both directions at IO.

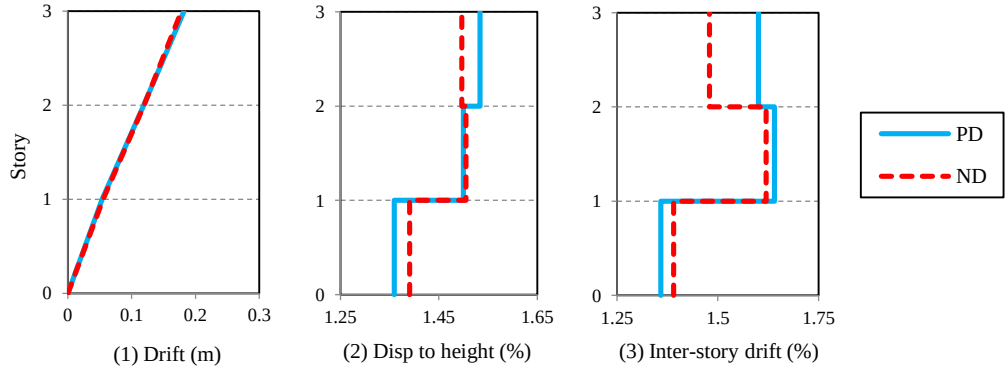

Fig. 12 Results of story drift for three-story steel frame with lateral loading pattern in both directions at LS.

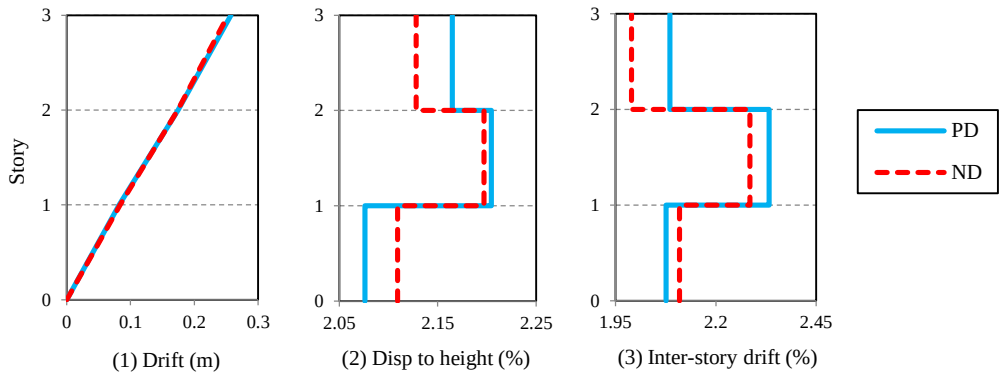

Fig. 13 Results of story drift for three-story steel frame with lateral loading pattern in both directions at CP.

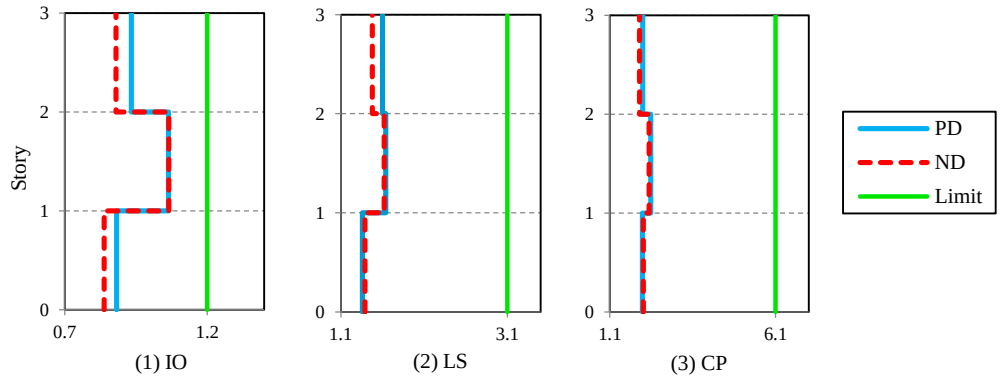

Fig. 14 Comparison of inter-story drift ratios (%) and their permitted values for three-story steel frame with lateral loading pattern in both directions.

3.2. Nine-story, five-bay steel frame

A nine-story five-bay steel frame with a set-back in height was considered as the second example for a PBD optimization problem. Fig. 15 shows the grouping of elements and applied loads for the frame.

A constant gravity load of W_1 = 32 kN/m was applied to the first to eighth stories and a constant gravity load of W_2 = 28.7 kN/m was applied to the beams of the roof. The seismic weight for the first story and roof was 1111 kN and 1176 kN, respectively, and for each of the second to eighth stories was 1092 kN. Fig. 16 shows the number of potential plastic hinges. The results of optimal sections and the best, worst, average, standard deviation and coefficient of variation of the structure weights are presented in Table 3.

Fig. 17 indicates the ratio of the best solution to those obtained from optimization algorithms for 20 independent runs. Fig. 18 compares the optimization convergence process of algorithms for a nine-story steel frame. Fig. 19 and 20 show the plastic hinge formation patterns for the optimal solution of the nine-story frame with lateral loading pattern in positive and negative directions at CP performance level, respectively. Fig. 21 illustrates the plastic hinge rotations to their allowable values in FEMA 356 for the nine-story frame with lateral loading pattern in both directions.

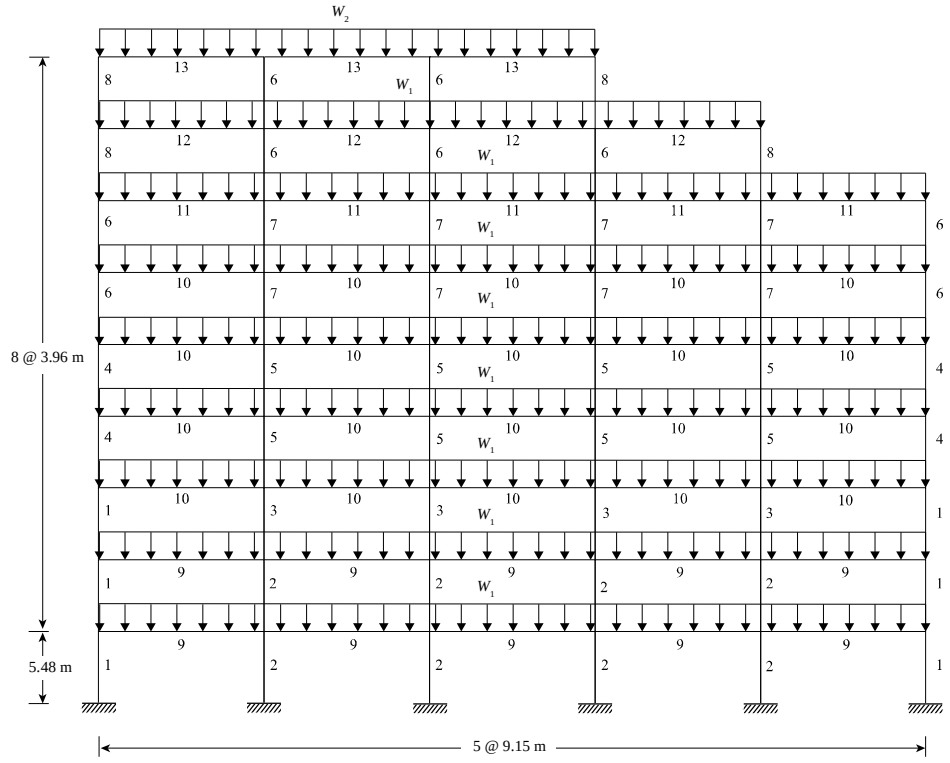

Fig. 15 Geometry, loading and grouping of the elements of nine-story steel frame with set-back in height

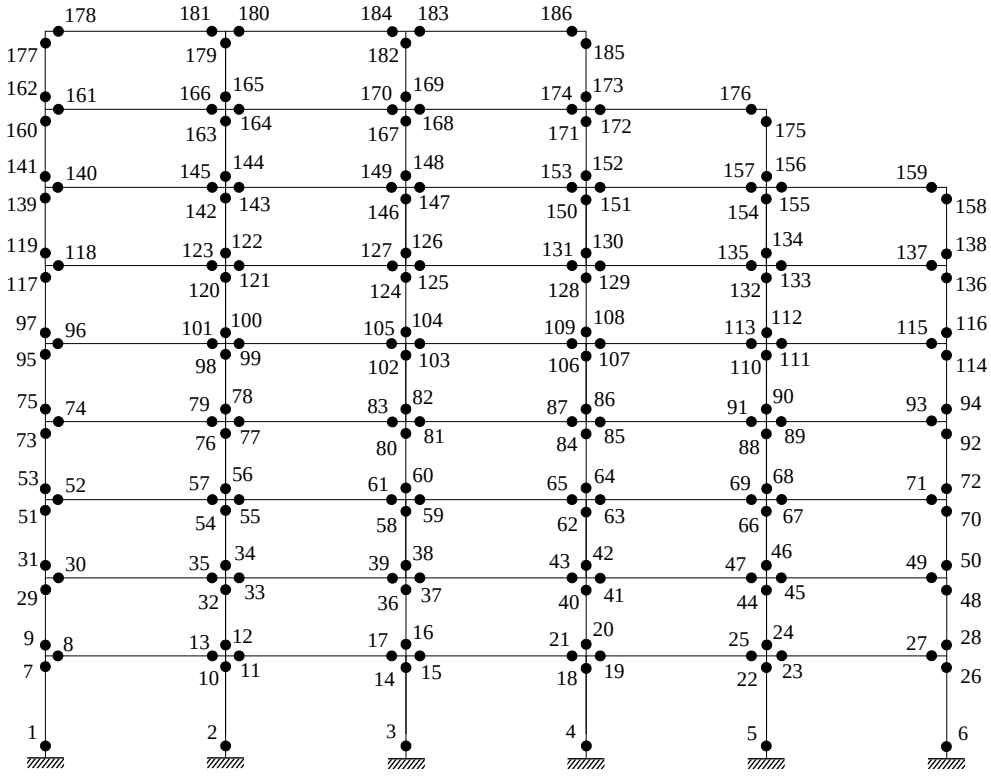

Fig. 16 Number of potential plastic hinges in nine-story steel frame

Table 3 Optimal sections and weights for nine-story steel frame.

Element group	WEO	AWEO
1	W 14 × 730	W 14 × 730
2	W 14 × 730	W 14 × 730
3	W 14 × 730	W 14 × 665
4	W 14 × 730	W 14 × 730
5	W 14 × 730	W 14 × 665
6	W 14 × 730	W 14 × 665
7	W 14 × 730	W 14 × 665
8	W 14 × 311	W 14 × 193
9	W 30 × 108	W 40 × 431
10	W 21 × 93	W 40 × 331
11	W 12 × 190	W 14 × 99
12	W 36 × 194	W 12 × 230
13	W 40 × 249	W 40 × 278
Best weight (kN)	2880.21	3771.74
Worst weight (kN)	5475.28	5541.20
Average weight (kN)	4558.56	4785.43
Standard deviation of weights (kN)	595.88	540.59
Coefficient of variations (%)	12.88	11.30

Fig. 22, 23 and 24 show the displacement of stories, displacement-to-height ratio, and inter-story drift ratio of the structure for both load patterns at IO, LS and CP, respectively. Fig. 25 illustrates the comparison of the inter-story drift ratios and their permitted values for the best solution of a nine-story steel frame.

4. Conclusions

In the current study, the optimum performance-based design of two steel frames with a set-back in height has been investigated. The structures were analyzed with lateral loading pattern based on the first mode shape in two directions using a new proposed procedure. The constraints considered are based on the acceptance criteria for steel moment frames according to FEMA-356 at each performance level. The implementation of the second stage depends on satisfying the constraints in the first stage. The WEO and AWEO algorithms were used to optimize the problems. The results showed the algorithms achieved the desired answers and had an appropriate performance to find the optimal solutions. The optimal weight values of three- and nine-story frames are 125.44 kN and 2880.21 kN, respectively. The results of plastic hinge formation and their rotation values confirmed that nonlinear static analyses should be performed in both directions for these types of frames.

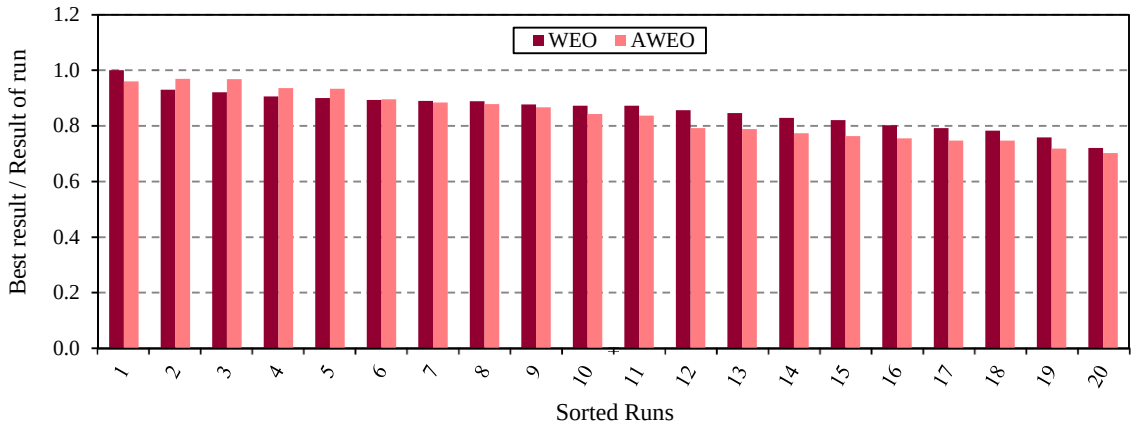

Fig. 17 Ratio of best solution to solution of each algorithm for nine-story steel frame.

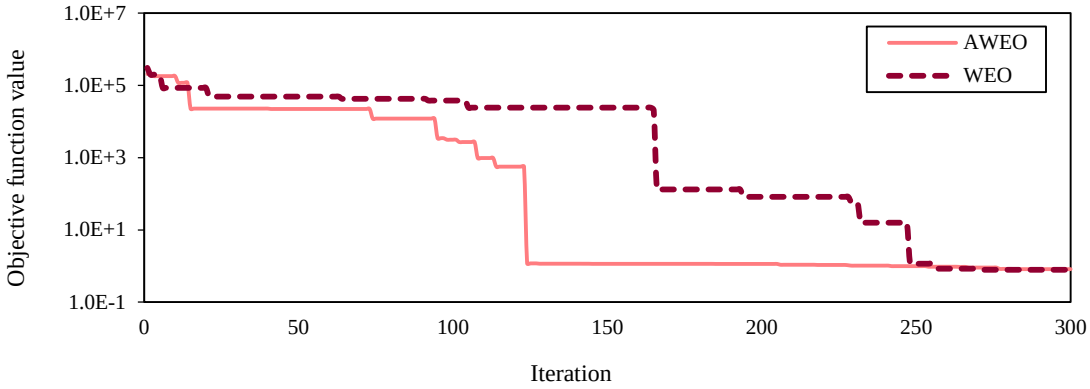

Fig. 18 Convergence curve of best solution of each algorithm for nine-story steel frame.

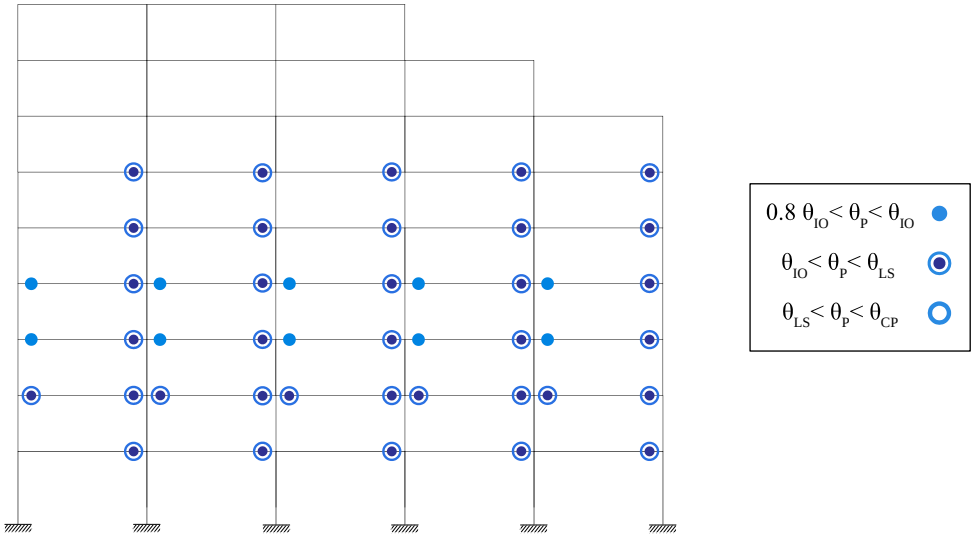

Fig. 19 Plastic hinges formation for nine-story frame with lateral loading pattern in positive direction at CP.

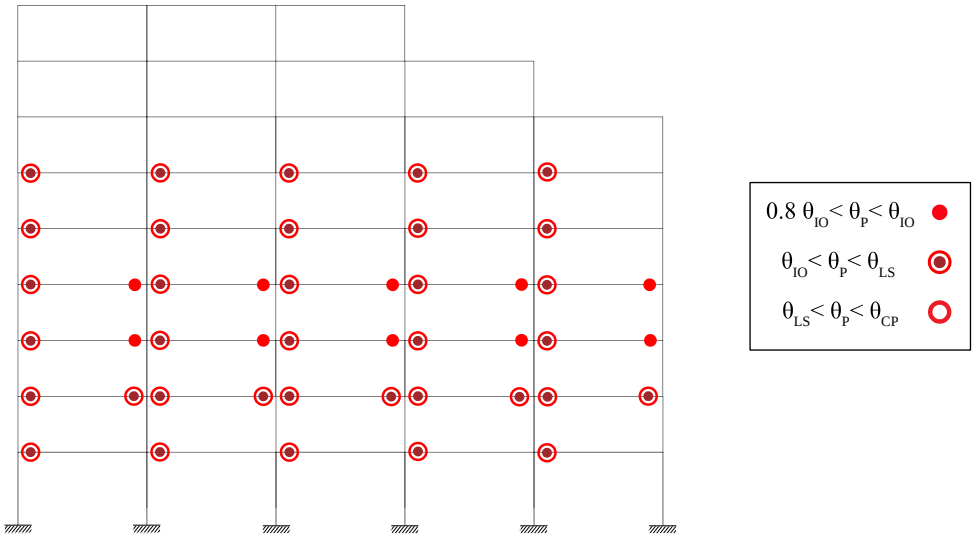

Fig. 20 Plastic hinges formation for nine-story frame with lateral loading pattern in negative direction at CP.

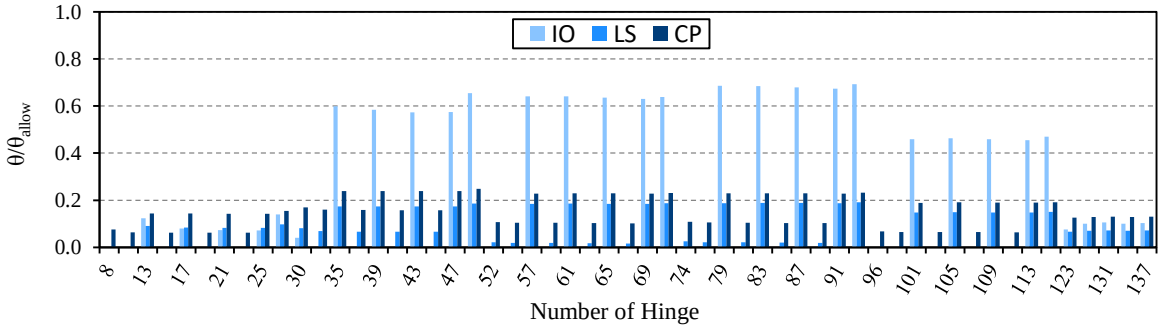

(a)

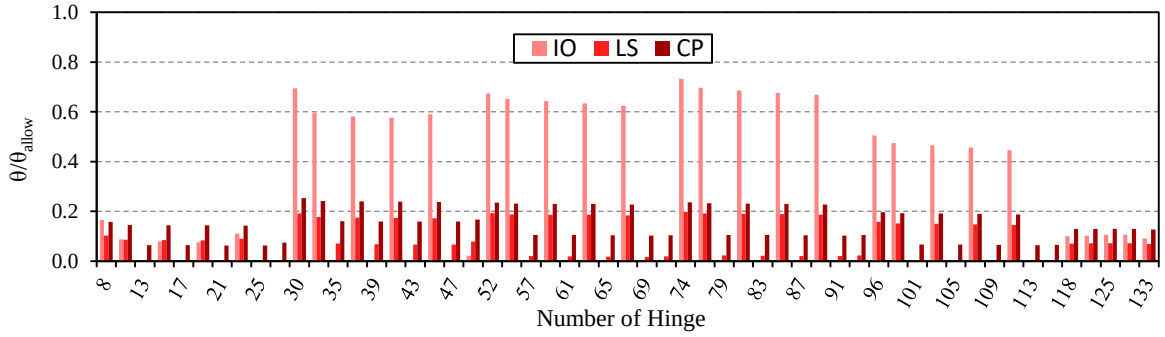

(b)

Fig. 21 Ratio of plastic hinges rotation to their allowable values for nine-story steel frame with lateral loading pattern in: (a) positive direction; (b) negative direction.

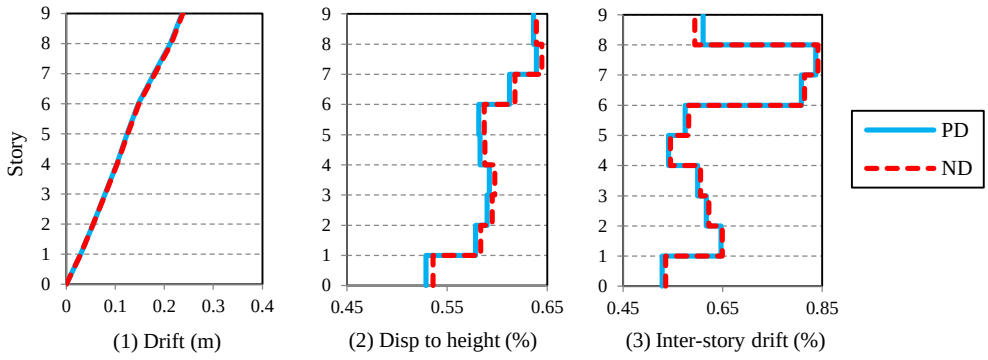

Fig. 22 Results of story drift for nine-story frame with lateral loading pattern in both directions at IO.

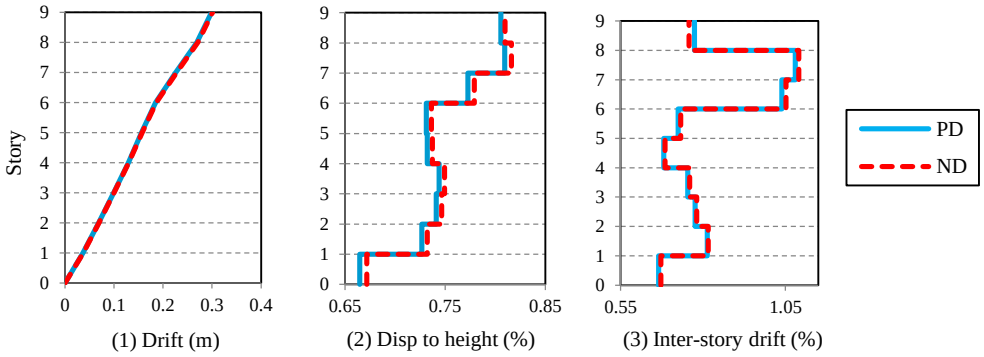

Fig. 23 Results of story drift for nine-story frame with lateral loading pattern in both directions at LS.

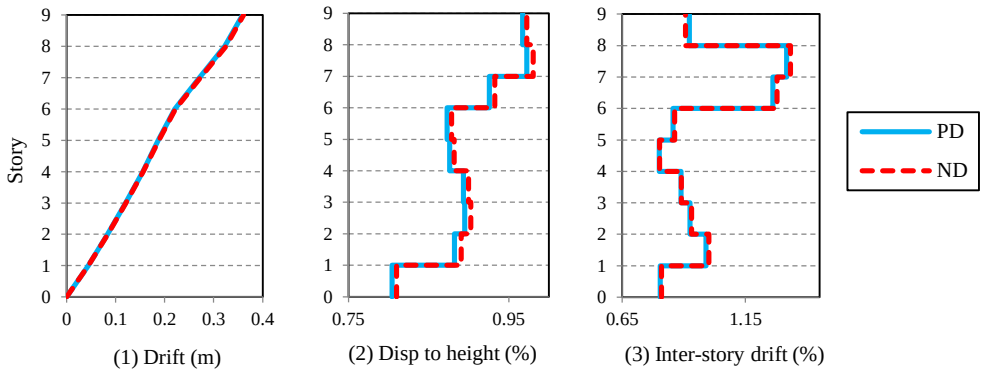

Fig. 24 Results of story drift for nine-story frame with lateral loading pattern in both directions at CP.

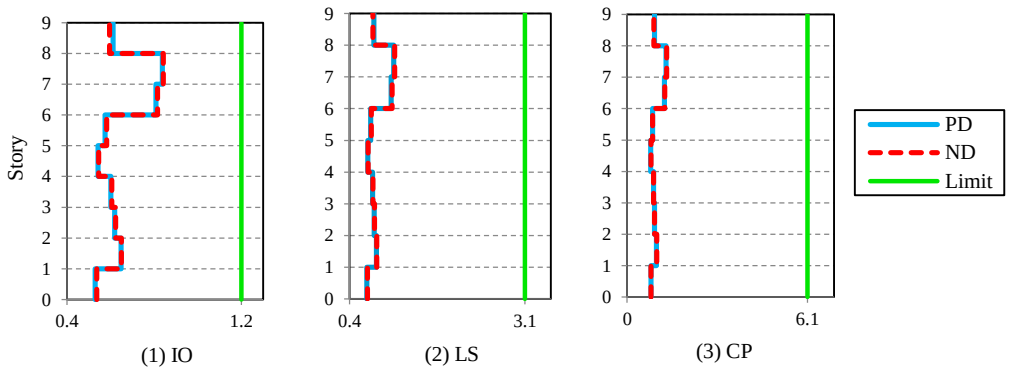

Fig. 25 Comparison of inter-story drift ratios (%) and their permitted values for nine-story steel frame with lateral loading pattern in both directions.

REFERENCES

[1] Kaveh, A. (2014), "Advances in metaheuristic algorithms for optimal design of structures", Springer,

[2] Kaveh, A. (2017), "Applications of metaheuristic optimization algorithms in civil engineering", Springer,

[3] Arjmand, M., Sheikhi Azqandi, M. and Delavar, M. (2018). "Hybrid Improved Dolphin Echolocation and Ant Colony Optimization for Optimal Discrete Sizing of Truss Structures." Journal of Rehabilitation in Civil Engineering, Vol. 6(1), pp. 70-87, https://doi.org/10.22075/jrce.2017.11367.1186

[4] Kaveh, A., Dadras, A. and Montazeran, A. (2018). "Chaotic enhanced colliding bodies algorithms for size optimization of truss structures." Acta Mechanica, Vol. 229(7), pp. 2883-2907, https://doi.org/10.1007/s00707-018-2149-8

[5] Kaveh, A., Hoseini Vaez, S. R. and Hosseini, P. (2018). "Matlab code for an enhanced vibrating particles system algorithm." International Journal of Optimization in Civil Engineering, Vol. 8(3), pp. 401-414,

[6] Kaveh, A., Vaez, S. R. H. and Hosseini, P. (2018). "Simplified dolphin echolocation algorithm for optimum design of frame." Smart Structures and Systems, Vol. 21(3), pp. 321-333,

[7] Choopan, Y. and Emami, S. (2019). "Optimal Operation of Dam Reservoir Using Gray Wolf Optimizer Algorithm (Case Study: Urmia Shaharchay Dam in Iran)." Journal of Soft Computing in Civil Engineering, Vol. 3(3), pp. 47-61, https://dx.doi.org/10.22115/scce.2020.189429.1112

[8] Mirzaei, B., Nasrollahi, K., Yousefbeik, S., Ghodrati Amiri, G. and Zare Hosseinzadeh, A. (2019). "A Two-Step Method for Damage Identification and Quantification in Large Trusses via Wavelet Transform and Optimization Algorithm." Journal of Rehabilitation in Civil Engineering, Vol. 7(1), pp. 1-20, https://doi.org/10.22075/jrce.2017.11678.1197

[9] Fathali, M. A., Dehghani, E. and Hoseini Vaez, S. R. (2020). "An approach for adjusting the tensile force coefficient in equivalent static cable-loss analysis of the cable-stayed bridges." Structures, Vol. 25, pp. 720-729, https://doi.org/10.1016/j.istruc.2020.03.054

[10] Gholizadeh, S., Danesh, M. and Gheyratmand, C. (2020). "A new Newton metaheuristic algorithm for discrete performance-based design optimization of steel moment frames." Computers & Structures, Vol. 234, pp. 106250, https://doi.org/10.1016/j.compstruc.2020.106250

[11] Hoseini Vaez, S. R., Mehanpour, H. and Fathali, M. A. (2020). "Reliability assessment of truss structures with natural frequency constraints using metaheuristic algorithms." Journal of Building Engineering, Vol. 28, pp. 101065, https://doi.org/10.1016/j.jobe.2019.101065

[12] Emami, H. and Emami, S. (2021). "Application of Whale Optimization Algorithm Combined with Adaptive Neuro-Fuzzy Inference System for Estimating Suspended Sediment Load." Journal of Soft Computing in Civil Engineering, Vol. 5(3), pp. 1-14, https://dx.doi.org/10.22115/scce.2021.281972.1300

[13] Kumar, P., Pandey, S. and Maiti, P. R. (2021). "A Modified Genetic Algorithm in C++ for Optimization of Steel Truss Structures." Journal of Soft Computing in Civil Engineering, Vol. 5(1), pp. 95-108, https://dx.doi.org/10.22115/scce.2021.242552.1249

[14] Gholizadeh, S., Kamyab, R. and Dadashi, H. (2013). "Performance-based design optimization of steel moment frames." Int J Optim Civil Eng, Vol. 3(2), pp. 327-343,

[15] Kaveh, A. and Nasrollahi, A. (2014). "Performance-based seismic design of steel

frames utilizing charged system search optimization." Applied Soft Computing, Vol. 22, pp. 213-221, https://doi.org/10.1016/j.asoc.2014.05.012

[16] Gholizadeh, S. (2015). "Performance-based optimum seismic design of steel structures by a modified firefly algorithm and a new neural network." Advances in Engineering Software, Vol. 81, pp. 50-65, https://doi.org/10.1016/j.advengsoft.2014.11.003

[17] FEMA-356. (2000), "Prestandard and commentary for the seismic rehabilitation of buildings", Federal Emergency Management Agency, Washington, DC.

[18] Gholizadeh, S. and Poorhoseini, H. (2016). "Seismic layout optimization of steel braced frames by an improved dolphin echolocation algorithm." Structural and Multidisciplinary Optimization, Vol. 54(4), pp. 1011-1029, https://doi.org/10.1007/s00158-016-1461-y

[19] Gholizadeh, S. and Baghchevan, A. (2017). "Multi-objective seismic design optimization of steel frames by a chaotic meta-heuristic algorithm." Engineering with Computers, Vol. 33(4), pp. 1045-1060, https://doi.org/10.1007/s00366-017-0515-0

[20] Mansouri, I., Soori, S., Amraie, H., Hu, J. W. and Shahbazi, S. (2018). "Performance based design optimum of CBFs using bee colony algorithm." Steel and Composite Structures, Vol. 27(5), pp. 613-622, https://doi.org/10.12989/scs.2018.27.5.613

[21] Gholizadeh, S. and Fattahi, F. (2018). "Damage-controlled performance-based design optimization of steel moment frames." The Structural Design of Tall and Special Buildings, Vol. 27(14), pp. e1498, https://doi.org/10.1002/tal.1498

[22] Karimi, F. and Hoseini Vaez, S. R. (2019). "Two-stage optimal seismic design of steel moment frames using the LRFD-PBD method." Journal of Constructional Steel Research, Vol. 155, pp. 77-89, https://doi.org/10.1016/j.jcsr.2018.12.023

[23] Fathali, M. A. and Hoseini Vaez, S. R. (2020). "Optimum performance-based design of eccentrically braced frames." Engineering Structures, Vol. 202, pp. 109857, https://doi.org/10.1016/j.engstruct.2019.109857

[24] Gholizadeh, S., Hassanzadeh, A., Milany, A. and Ghatte, H. F. (2020). "On the seismic collapse capacity of optimally designed steel braced frames." Engineering with Computers, Vol., pp. https://doi.org/10.1007/s00366-020-01096-7

[25] Kaveh, A., Farahmand Azar, B., Hadidi, A., Rezazadeh Sorochi, F. and Talatahari, S. (2010). "Performance-based seismic design of steel frames using ant colony optimization." Journal of Constructional Steel Research, Vol. 66(4), pp. 566-574, https://doi.org/10.1016/j.jcsr.2009.11.006

[26] Talatahari, S., Hosseini, A., Mirghaderi, S. and Rezazadeh, F. (2014). "Optimum performance-based seismic design using a hybrid optimization algorithm." Mathematical Problems in Engineering, Vol. 2014, pp.

[27] Gholizadeh, S. and Milani, A. (2016). "Optimal performance-based design of steel frames using advanced metaheuristics." Journal of Civil Engineering, Vol. 17, pp. 607-623,

[28] Gholizadeh, S. and Poorhoseini, H. (2016), "Performance-Based Optimum Seismic Design of Steel Dual Braced Frames by Bat Algorithm", In: Metaheuristics and Optimization in Civil Engineering, Springer International Publishing, Cham, pp. 95-114.

[29] Gholizadeh, S. and Ebadijalal, M. (2017). "SEISMIC DESIGN OPTIMIZATION OF STEEL STRUCTURES BY A SEQUENTIAL ECBO ALGORITHM." International Journal of Optimization in Civil Engineering, Vol. 7(2), pp. 157-171,

[30] Gholizadeh, S. and Ebadijalal, M. (2018). "Performance based discrete topology optimization of steel braced frames by a new metaheuristic." Advances in

Engineering Software, Vol. 123, pp. 77-92, https://doi.org/10.1016/j.advengsoft.2018.06.002

[31] Fakhraddini, A., Fadaee, M. J. and Saffari, H. (2019). "A Target Displacement for Pushover Analysis to Estimate Seismic Demand of Eccentrically Braced Frames." Journal of Rehabilitation in Civil Engineering, Vol. 7(3), pp. 103-116, https://doi.org/10.22075/jrce.2018.13427.1245

[32] Babaei, M. and Moniri, A. (2018). "Use of Tuned Mass Dampers in Controlling the Vibrations of Steel Structures with Vertical Irregularity of Mass." Computational Engineering and Physical Modeling, Vol. 1(2), pp. 83-94, https://dx.doi.org/10.22115/cepm.2018.137303.1035

[33] Chabokan, E. and Faridmehr, I. (2018). "Seismic Assessment of Steel Moment Frames with Irregularity in Mass and Stiffness." Computational Engineering and Physical Modeling, Vol. 1(4), pp. 71-89, https://dx.doi.org/10.22115/cepm.2018.141604.1039

[34] LRFD-AISC. (2001), "Manual of steel construction- load and resistance factor design", In: LRFD-AISC, American Institute of Steel Construction (AISC), Chicago, Illinois, USA, pp.

[35] Grierson, D. E., Gong, Y. and Xu, L. (2006). "Optimal performance-based seismic design using modal pushover analysis." Journal of Earthquake Engineering, Vol. 10(01), pp. 73-96,

[36] Cimagala, J. P. (2021). "Optimization of Reduced Beam Sections (RBS) for Ductile Detailing of Seismic Joint Connections Using Finite Element Analysis (FEA)." Computational Engineering and Physical Modeling, Vol. 4(3), pp. 43-54, https://dx.doi.org/10.22115/cepm.2021.273581.1153

[37] Gong, Y. (2003), "Performance-based design of steel building frameworks under seismic loading", Ph.D. Thesis, University of Waterloo, Waterloo, Ontario, Canada.

[38] Kaveh, A. and Bakhshpoori, T. (2016). "Water Evaporation Optimization: A novel physically inspired optimization algorithm." Computers & Structures, Vol. 167, pp. 69-85, https://doi.org/10.1016/j.compstruc.2016.01.008

[39] Kaveh, A. and Bakhshpoori, T. (2016). "An accelerated water evaporation optimization formulation for discrete optimization of skeletal structures." Computers & Structures, Vol. 177, pp. 218-228, https://doi.org/10.1016/j.compstruc.2016.08.006

[40] Chopra, A. K. and Goel, R. K. (2002). "A modal pushover analysis procedure for estimating seismic demands for buildings." Earthquake Engineering & Structural Dynamics, Vol. 31(3), pp. 561-582, https://doi.org/10.1002/eqe.144